COeCO: A new β-delayed conversion-electron spectroscopy setup for low-energy ISOL beams at the ALTO facility in Orsay

G Tocabens, C Delafosse, D Verney, E Cantacuzène, M. Cheikh Mhamed, I Deloncle, F Didierjean, W Dong, C Gaulard, B Genolini, et al.

COeCO : A new β-delayed conversion-electron spectroscopy setup for low-energy ISOL beams at the ALTO facility in Orsay

G. Tocabens[a], C. Delafosse[a], D. Verney[a,*], E. Cantacuzène[a], M. Cheikh Mhamed[a], I. Deloncle[a], F. Didierjean[b], W. Dong[a], C. Gaulard[a], B. Genolini[a], J. Guillot[a], F. Hammache[a], S. Harrouz[a], F. Ibrahim[a], H. Jacob[a], M. Kaci[a], A. de Lara[a], N. de Séréville[a], F. Le Blanc[a], M. Lebois[a,c], R. Lozeva[a], I. Matea[a], B. Roussière[a], A. Segovia-Miranda[a], R. Thoër[a]

[a] *Université Paris-Saclay, CNRS/IN2P3, IJCLab, 91405, Orsay, France*
[b] *Université de Strasbourg, CNRS, IPHC UMR 7178, 67000, Strasbourg, France*
[c] *Institut Universitaire de France, 1 Rue Descartes, 75005, Paris, France*

Abstract

A new β-decay station, COnversion electrons Chasing at Orsay (COeCO), has been developed at ALTO to perform conversion electron spectroscopy studies of neutron-rich nuclei produced by photo-fission of a uranium carbide target. It is based on the collection of a low-energy ISOL beam on a mylar tape, and the transportation of the electrons emitted by the produced radioactive source through a magnetic field induced by two copper coils, towards a cooled Si(Li) detector. In this article, a detailed description of the new decay station and its components is given. The magnetic field induced by the coils was measured and compared to simulations performed with the COMSOL® software. The efficiency of the detection setup was estimated using a ^{207}Bi and a ^{152}Eu source as an off-line commissioning. Finally, the results obtained with a ^{96}Rb radioactive beam for the on-line commissioning are presented.
Keywords: conversion-electron spectroscopy, magnetic transporter, β-decay, half-life measurements

1. Introduction

Internal conversion electron spectroscopy is of utmost importance when studying nuclear structure, as it not only allows spin and parity assignment, through the determination of the multipolarity of a given transition, but also is the best tool to study electric monopole transitions – E0. Such transitions can occur between states of same spin and parity and are the only possible transition in the case of two 0^+ states. It has been shown that a large E0 transition strength ρ_0, which is directly linked to a change in mean-square charge radius, usually indicates strong shape mixing [1]. Experimentally, ρ_0 is inversely proportional to the lifetime of the considered transition, which contains the nuclear structure information, and an electronic factor, Ω, which can be computed theoretically [2]. The observation of an electric monopole transition must thus coincide with the measurement of its lifetime.

In order to perform conversion electron spectroscopy, several ISOL facilities equipped themselves with dedicated spectrometers, with different experimental strategies in mind, either looking to increase the efficiency of the system [3, 4] or its selectivity [5, 6]. In this context, we decided to develop a new decay station at ALTO[1] [7] on the model of ELLI[2] [5], to increase the selectivity of the existing measurement setup and allow the study of short-lived nuclei via β-decay.

In the former configuration, the radioactive beam produced by photo-fission of ^{238}U was collected on a mylar tape to produce a radioactive source. This source was then moved to the detection apparatus made of a plastic scintillator for β-tagging, a High-Purity Germanium (HPGe) detector for γ-spectroscopy and a Si(Li) detector for conversion electron spectroscopy in a very compact geometry. This configuration was for example used in 2013 in an experiment dedicated to the study of ^{80}Ge, see [8] for a thorough depiction of the setup. The development of the new decay station aims to tackle both limitations imposed by this geometry and observed at the time. First, the two steps collection-detection process implies that short-lived nuclei are not easily studied, as the tape takes a full second to move the source. Then, the very close proximity of the detectors from the source induces a huge background coming from Compton scattered γ-rays leaving some energy deposit in the Si(Li) detector. The new decay station is designed so that both collection and detection happen at the same point, reemploying the three types of detectors the old system was equipped with.

In the following, all components of COeCO will be thoroughly described, and the simulations performed as a proof of concept of the detection system will be presented. The last sections of this article concentrate on the commissioning of COeCO, both off-line using standard cal-

*Corresponding author
Email address: verney@ijclab.in2p3.fr (D. Verney)
[1] Accélérateur Linéaire et Tandem d'Orsay
[2] Electron Lens for IGISOL

ibration sources and on-line, by collection of neutron-rich Rb beams.

2. Characteristics of COeCO

COeCO is based on a magnetic transporter – see Section 3.2 – so that the beam is collected on the tape while the Si(Li) detector is moved away from it. Conversion electrons emitted by the radioactive source are transported following the magnetic field lines towards the detector, whereas γ-rays are not, reducing Compton background. A HPGe detector is placed close to the source for γ-ray spectroscopy and a plastic scintillator surrounds the tape at the collection point, see Figures 1 and 2.

The system is composed of two magnetic coils close to the Helmholtz configuration, where the aperture of the coils is roughly the same as the distance between them. It was previously shown for the ELLI spectrometer, that the optimum position for both the source and the detector are in the center of the coils. Thus, the tape runs in the middle of the first coil, and the Si(Li) detector is placed in the center of the second coil, as portrayed Figure 2. In the true Helmholtz configuration, the magnetic field along the axis between the center of the coils presents a plateau in the middle. This is particularly important not to lose electrons emitted by the source when they follow the field lines towards the detector. This is however not achievable if the beam is to be collected in the center of the first coil, and in the chosen configuration, the magnetic field along the symmetry axis of the system shows a significant drop of 9.10^{-2} T in the space between the coils, see Figure 6.

The beam is coming through a small tube on the side of the chamber, oriented at 45° so that it can come between the coils. A smaller angle would imply a larger distance between the coils, hence a smaller efficiency for coils of the same size. A bigger angle would produce a broader source on the tape, and the risk to collect the beam outside the tape – a beam of 5 mm diameter would imply a source of 7 mm at the collection point, which is just enough to be completely collected on the 8 mm wide mylar tape.

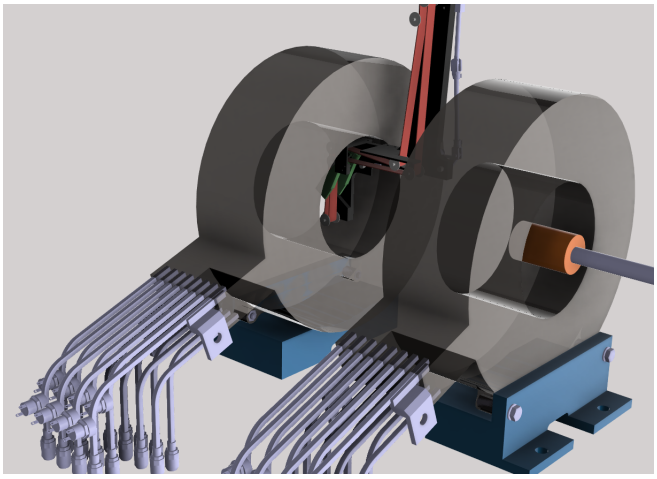

Figure 1: CAD of the interior of the main chamber. The mylar tape, in red, and the plastic scintillator, in green, are both held by an aluminum arm, in black. The Si(Li) detector, in orange, is facing the mylar tape.

A 1.2-mm thin aluminum window closes the chamber on the left side to make room for a HPGe detector as close to the source as possible. This window can be removed to allow for easy access to the tape and its holding mechanics in case of a break or jam of the tape system. A plastic scintillator completes the detection system. It is made of two square-shape scintillating parts, connected to a PMT via optic fibres, as explained later in Section 3.1. A CAD of the interior of the chamber and the magnetic coils surrounding it is visible on Figure 1.

A retractable Faraday cup can be positioned in front of the beam, right next to the collection region on the tape surface, and removed using a system of ball-and-socket joints. This allows for beam tuning before sending it to the tape, even though by construction, the cup can only be inserted a few millimeters away from the tape. Finally, a calibration source is attached at the end of a rod, enabling it to be moved under vacuum and positioned as close to the beam collection point as possible. When inserted, the source is located two centimeters in front of the collection point, on the axis made by the collection point and the Si(Li) detector.

The main detector of the system is a lithium compensated silicon N-I-P diode, model ESLB from Canberra. It is made of a thin gold layer – 20 to 40 $\mu g/cm^2$ – on the front P-side face. The rear face is a lithium doped N-side of roughly 300 μm. The total depletion depth is 3000 μm when fully depleted, at −300 V, which allows for detection of electrons up to 1.7 MeV, with a resolution of 3.3 keV at 975 keV measured with a ^{207}Bi source, see Figure 9, a). The detector is mounted on a cold finger to cool it to liquid nitrogen temperature, with a small dewar built at IJCLab [3] attached to its end. The whole is fixed on a linear translator to move the detector backwards behind a valve and separate it from the rest of the chamber, where the tape runs. This can also be used to optimize the position of the front-face of the detector inside the chamber and slightly adjust the efficiency curve of the system.

Vacuum in the chamber is maintained using three turbo pumps and a cryogenic trap. The three pumping spots are placed on top of the tape station, twenty centimeters downwards from the chamber, and in the back of the Si(Li) liquid nitrogen dewar. The two last ones can be separated from the chamber by two valves if any intervention needs to be done inside the chamber. By filling the cryogenic trap with liquid nitrogen, a vacuum of 8.7×10^{-7} mbar could be attained in the chamber during the first measurement campaign. This also traps impurities avoiding their accumulation on the surface of the detector that leads to a degradation of its resolution while potentially damaging it permanently.

[3] Laboratoire de Physique des 2 Infinis Irène Joliot-Curie

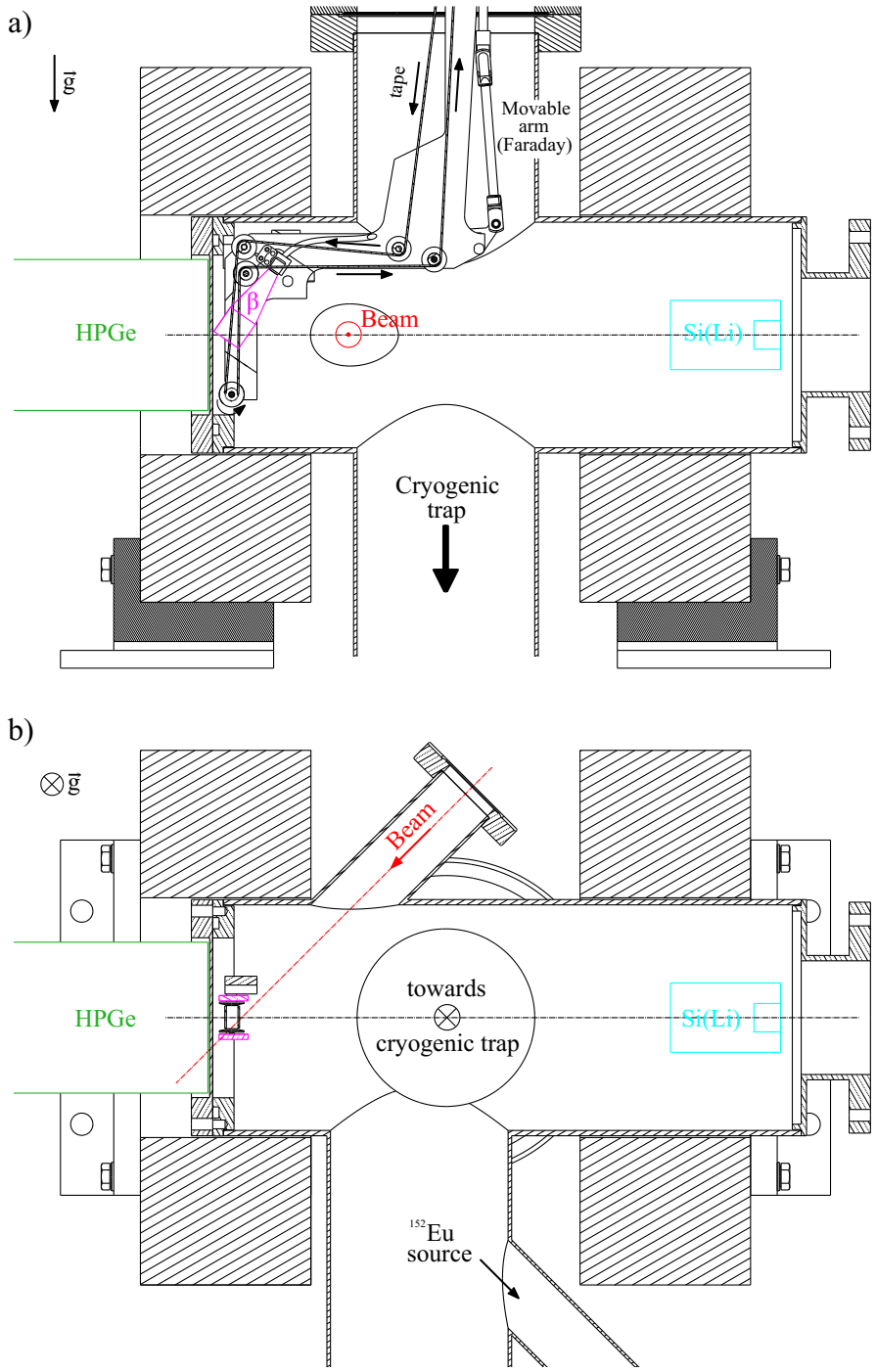

Figure 2: Cutaway of the setup as viewed from the side – a) – and from the top – b). Both coils are hatched on the scheme, the tape and the Si(Li) detector placed in the center of each. One of the components of the plastic scintillator – see Section 3.1 – is visible surrounding the tape at the collection point of the beam.

3. COeCO components

3.1. The β plastic scintillator

In order to detect the β electrons emitted by the collected radioactive beams in a compact geometry, a new detector was developed at IJCLab, see a schematic view on Figure 3. It is made of two $17\times17\times3$ mm^3 BC-400 plastic scintillators [9] components, coupled to a PMT through optical fibers. The thickness of the plastic was selected so that 1-MeV electrons lose their energy in it, while γ-rays interaction probability remains negligible. To ensure maximum light collection, the active parts are connected to seven 1-mm diameter optical fibers, using a 30-mm high parallelepipedic piece to follow recommendations on the

aperture angle summarized in [10]. At the end of the optical fibers, a 1-mm thin silicon disc is used to ensure optical coupling to the entrance window of the PMT (Hamamatsu R7400U-01 [11]), placed 10 cm above the first magnetic coil. It is a grid-based PMT of eight stages and is not affected by the field surrounding it at this distance from the coil, which is less than 5×10^{-2} T.

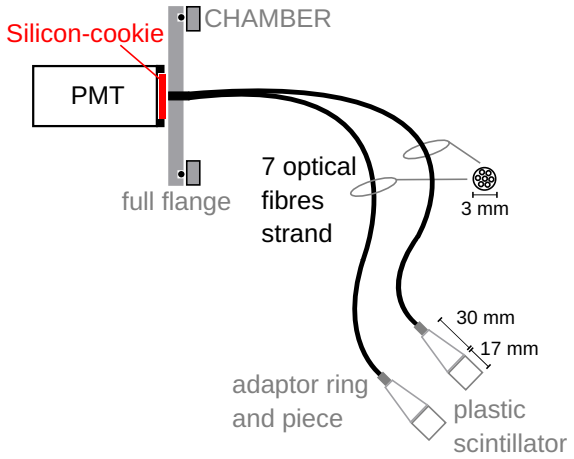

Figure 3: Sketch of all the components of the plastic scintillator detector for β-tagging.

The detector was characterized during the on-line commissioning of COeCO, detailed in Section 4. A source of ^{98}Rb formed by the collection of the beam provided by ALTO was used to determine its efficiency, obtained by comparing the area below the peaks in the direct spectra – γ and conversion electrons – and in the same spectra, β-gated. The final adopted value for the efficiency is 5 ± 1 %, as shown Figure 4. This low value is mostly explained by the geometry of the detector, which only covers a quarter of the total solid angle, as well as the several interfaces between the scintillation part of the detector and the PMT, that can be seen Figure 3.

3.2. Magnetic transporter

To ensure that the beam collection point and the measurement point are identical and therefore avoid the need of transport of the activity in front of the detector, a magnetic apparatus was designed. Its purpose is to allow the collection of the beam on the tape, while placing the Si(Li) far enough from the source, the conversion electrons being guided along the field lines towards the detector surface. By doing so, the angular coverage of the detector as viewed from the source spot is divided by a factor of roughly 2×10^3, reducing the background induced by γ-rays by the same factor. The tape motion is only used for the purpose of the evacuation of the long-lived daughter activities. To obtain a large energy acceptance, it was decided that the best design would be composed of two copper coils close to the Helmholtz configuration to avoid too large a drop in the magnetic field in the region between the coils that may cause a loss in the transport efficiency

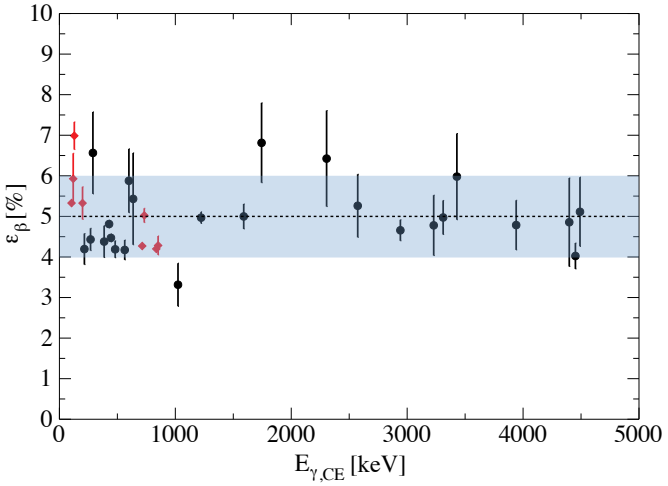

Figure 4: Efficiency of the β plastic scintillator, as a function of the observed γ transition – black dots – and electron transition – red diamonds. Mean adopted value is shown in dots, and its uncertainty in blue.

of the conversion electrons. In this configuration the maximum transmission is achieved when the beam is collected in the center of the first coil and the Si(Li) detector is placed in the center of the second one.

The magnetic field induced by the two coils was simulated using the COMSOL Multiphysics® program, which gives the adequate tools to compute magnetic fields, as well as study the behaviour of charged particles in said field [12]. A series of simulations were performed to dimension the coils with constraints on the integration of the detectors and the coils to the existing beamline, as well as on the power supply available – a 15 kW model *EA-PS-9080-510 3U* delivering up to 80 V and 510 A. The firm responsible for the manufacturing of the coils carried out additional studies on leakage field and hydraulic cooling and the final coils were built with 224 turns divided in 14 layers. This results in an inner diameter of 135 mm and thickness of 96 mm. Both coils are fixed on movable supports to vary the distance between them and are cooled by eight water circuits with a 0.66 L/min flow for heat dissipation. The full reports from the manufacturer, SEF Technologies, can be found in Appendix 2, pages 115-124 in [13].

The final geometry of the setup including the coils was imported to COMSOL® and the magnetic field computed using the *AC/DC* package of the software to produce a three dimensional mapping of the field, whose projection is given Figure 5. The magnetic field was measured using a Hall effect probe in several points on the central axis of the system – results are reported on Figure 6 – as well as on the coils themselves to check for any leak. All measures are consistent with the simulations within a 1 % range.

The total electron efficiency of COeCO mainly comes from the efficiency of the transport of the electrons from the mylar tape to the detector. This transport efficiency is influenced by the magnetic field induced by the coils, and

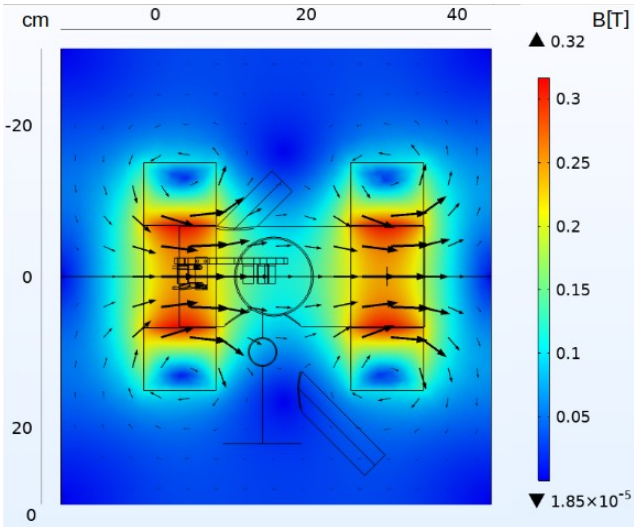

Figure 5: Two-dimensional projection of the magnetic field strength induced by the two coils simulated using COMSOL®. The field is symmetric by rotation around the axis formed by the center of both coils.

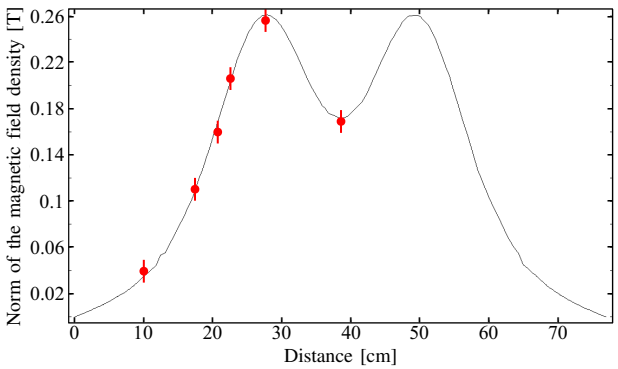

Figure 6: Simulated magnetic field along the symmetry axis of COeCO. The points show the measured values of the magnetic field.

thus their length, aperture diameter, the distance between them and the current flowing through the copper spires. Both the distance between the coils and the current sent through the spires can be changed in COeCO to change the efficiency slightly if needed.

Using the calculated magnetic field, an estimation of the transport efficiency of the electrons from the radioactive source to the Si(Li) detector was performed using the *particle tracing* package of COMSOL®. The transport efficiency is defined as the ratio between the number of electrons reaching the surface of the detector and the number of electrons emitted at the source. This ratio was studied by releasing 10^4 electrons from the center of the first coil randomly in 2π sr and counting how much reached a disc of 25.2 mm in diameter representing the detector. The results are reported in Figure 7 for electrons of energy ranging from 20 keV to 1800 keV, with a 20 keV step. The efficiency curve shows a decreasing behaviour with oscillations coming from the trajectories followed by the electrons in the magnetic field. Each local maximum corresponds to the focusing point of the trajectories being located on the detector for a given number of rotations in the magnetic field. Examples of electrons trajectories for two different energies are represented on Figure 8, with the number of rotations depending on the initial angle of the electron and its energy – the higher the energy, the less the spiralling.

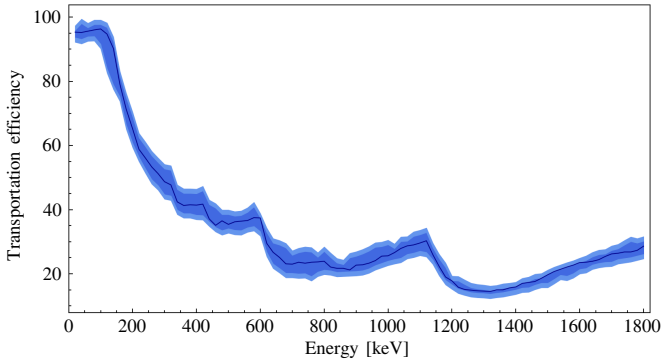

Figure 7: Calculated transport efficiency of electrons from the source to the Si(Li) detector. The first envelope is obtained by varying the position of the source by ±2 mm and the second, light blue one, comes from the uncertainty on the result of the simulations which is related to the meshing made in COMSOL®.

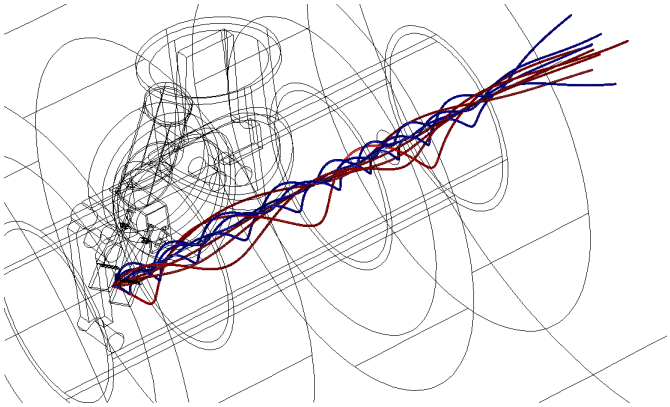

Figure 8: Example of trajectories of electrons emitted by a monoenergetic source of 200 keV, in blue, and 1200 keV, in red.

Given the geometry of the system, and the way the radioactive beam is collected on the mylar tape, the produced ions have to go through a small distance inside the magnetic field induced by the coils. This results in a small vertical deviation of the beam, of 4 mm for ions of mass 100 and 30 keV kinetic energy – the usual beam extraction energy at ALTO. Two electrostatic dipoles placed right before the main chamber allow to correct for this effect. This is particularly important as the ions must not be collected off the tape and create a second radioactive source, which would contribute to the spectral background. Moreover, a misalignment of the source from the symmetry axis of the system would result in a loss of transport efficiency.

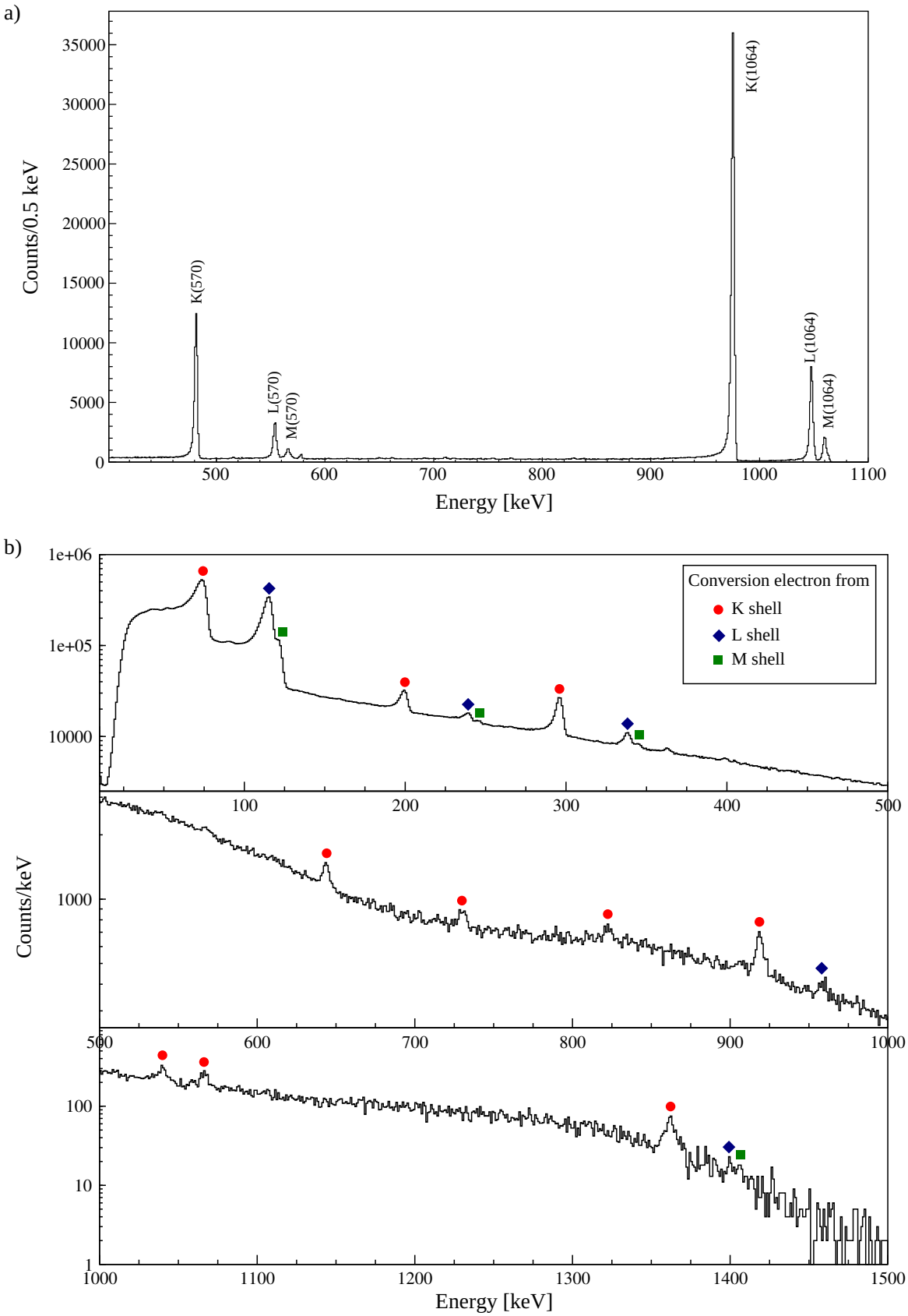

Figure 9: COeCO spectra taken with a source of a) ^{207}Bi and b) ^{152}Eu. The FWHM of the K transition at 975 keV was measured to be 3.3 keV, but depends a lot on how the detector is handled and the shielding from outside noise.

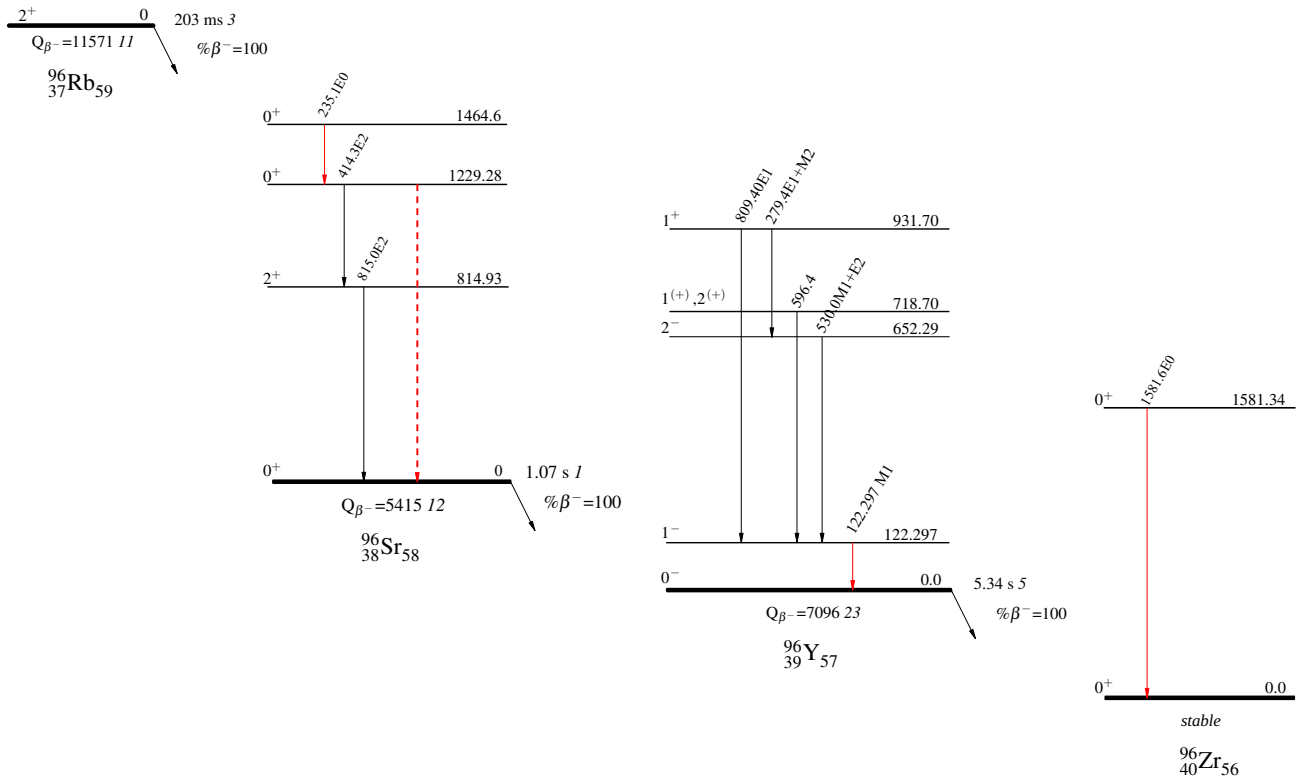

Figure 10: Decay chain from ^{96}Rb. The low-energy part of the decay schemes from the daughter nuclei are reported from ENSDF [14]. Transitions in red were observed in the conversion electron spectrum, and the red dotted line highlights the unobserved $0_2^+ \rightarrow 0_1^+$.

4. Commissioning of COeCO

The commissioning of the whole system was conducted in two parts. The first tests were done using two standard sources, ^{207}Bi and ^{152}Eu, to get converted transitions over all the energy range covered by the Si(Li) detector. Because of the space requirement for the β-detector, it is not possible to place a radioactive source directly on the mylar tape. A source holder was designed to insert, under vacuum, a calibration source as close as possible to the tape, roughly 2 cm in front of the collection point, on the symmetry axis of COeCO.

The second part of the commissioning was performed on-line, with radioactive beams, so that the source could be collected on the tape. This part of the commissioning was designed to study the main characteristics of COeCO and the possibilities it offers. γ-CE coincidence data sets were produced, as well as CE events time distributions allowing the extraction of half-lives of converted transitions – crucial quantities to compute transition strengths. This experiment was part of a larger campaign aimed at studying E0 transitions in the region of shape transition close to $N = 60$ in Sr and Zr isotopes [15]. Results from the decay of ^{96}Rb will be presented here, and results from the decays of $^{95-100}$Rb will be presented in a forthcoming publication.

4.1. Off-line commissioning

The efficiency of COeCO was computed for all converted transitions in both ^{207}Bi and ^{152}Eu, which spectra are visible Figure 9. The ^{152}Eu source, even though not standard for calibrating detectors dedicated to conversion electron spectroscopy, has very desirable characteristics. It allows to calibrate both the Si(Li) and the HPGe detectors at the same time, and covers the whole energy range accessible by the Si(Li) detector ($10 - 1700$ keV). All conversion coefficients are well-known, making it possible to calculate the absolute efficiency of COeCO as a function of the energy, while it is usually not the case with radioactive beams accessible at ALTO.

The obtained efficiency as a function of the energy is reported on Figure 12. Although the source is not placed on the optimal spot, the efficiency curve exhibits the same behaviour as expected from the simulation of the transmission, with localised maxima between 550 keV and 600 keV and around 1.1 MeV, and a decreasing trend, see Figure 7.

4.2. On-line commissioning

The second part of the commissioning consisted in the study of converted transitions in daughter nuclei populated in the decay of neutron-rich ^{96}Rb collected sources, mainly in ^{96}Sr and ^{96}Zr. The first excited state of ^{96}Zr is a 0^+ state located at 1581.6 keV excitation energy having a long half-life (38.0 ± 0.7 ns [16, 17, 18]), thus providing a good test case to measure half-lives with COeCO. In the case of ^{96}Sr, a strong E0 transition has already been observed from the decay of $0_3^+ \rightarrow 0_2^+$ at 235.1 keV [19]. The direct transition from the first excited 0_2^+ state to the

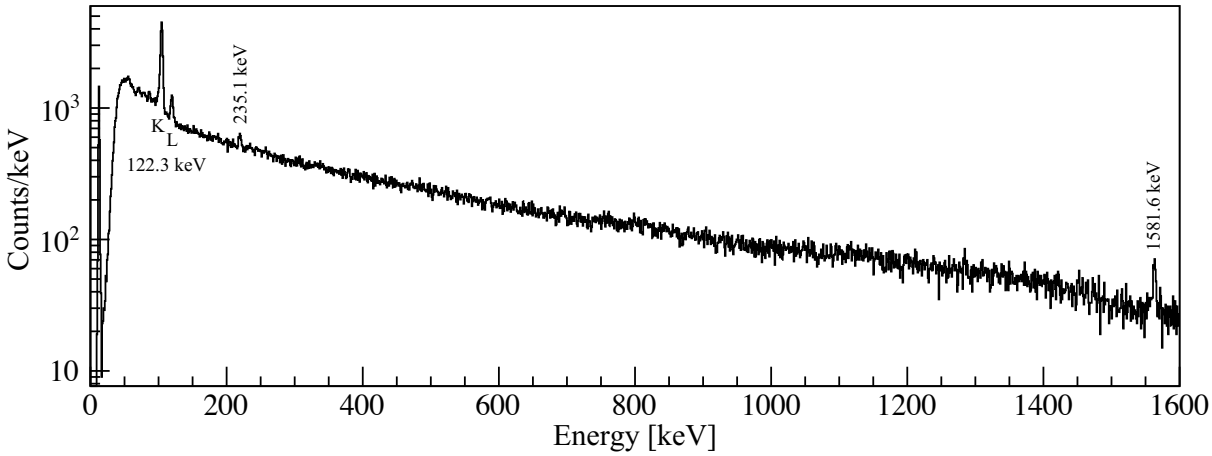

Figure 11: β-gated conversion electron spectrum obtained using a radioactive beam of ^{96}Rb collected on a movable mylar tape with the COeCO device. The measurement was done using a tape cycle of 2 s – 0.2 s collection and 1.8 s decay – for 1800 cycles in total.

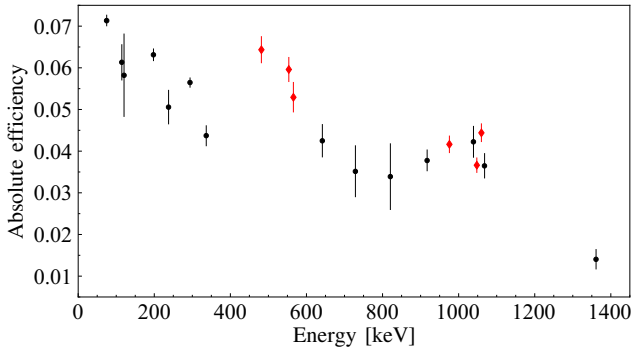

Figure 12: Efficiency of the COeCO setup measured with two sources of ^{152}Eu (black dots), and ^{207}Bi (red diamonds), placed at the source holder position.

ground state has long been unsuccessfully searched for, its observation would give useful insights on shape transition occurring in the region, see Figure 10.

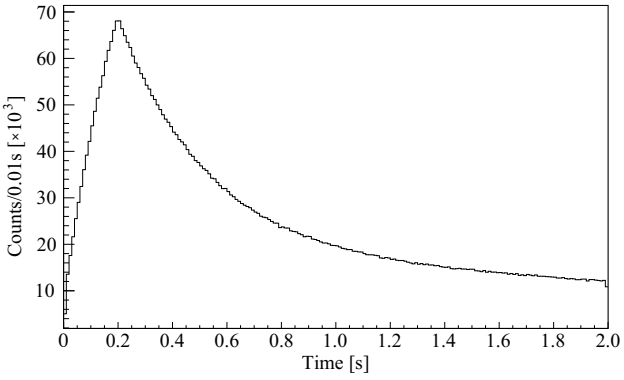

Figure 13: β-decay accumulated activity as a function of time. The rising part corresponds to the collection of the beam on the tape while the decay after 0.2 s to the beam being stopped for the measurement.

A beam of ^{96}Rb was obtained at ALTO from the photofission of a ^{238}U target using a primary beam of 50 MeV electrons. The fission products were then surface-ionised and separated at the PARRNe mass-separator, with a resolution of $M/\Delta M = 1500$ [20]. The obtained purified beam of ^{96}Rb was collected on a grounded Al-coated mylar tape for 0.2 s and the source was measured for 1.8 s before being removed to collect a new source, for cycles of 2 s in total, the total activity curve of the source can be seen Figure 13.

Table 1: Electron binding energies for the three daughter nuclei involved in the decay of ^{96}Rb, in eV, taken from [21].

Element	**K 1s**	**L1 2s**	**L2 2p$_{1/2}$**	**L3 2p$_{3/2}$**
Sr	16105	2216	2007	1940
Y	17038	2373	2156	2080
Zr	17998	2532	2307	2223

The β-gated conversion electron spectrum is shown in Figure 11. The chosen tape cycle allows the observation of transitions in the decay chain down to the stable ^{96}Zr : the M1 transition line fed by the decay of ^{96}Sr in ^{96}Y at 122.3 keV – both K and L components can be seen – as well as the E0 transition at 1581.6 keV in ^{96}Zr fed by the decay of ^{96}Y – all the involved electron binding energies are reported in Table 1. The only visible transition in ^{96}Sr fed by the decay of ^{96}Rb is the E0 transition at 235.1 keV, see Figures 10, 11.

All these transitions are already known, yet the only conversion electron spectroscopy of the decay of ^{96}Rb was published in the early eighties by G. Jung and collaborators [19] as part of a study of ^{96}Y. The present experiment allowed to observe for the first time γ lines in coincidence with the 235.1 keV E0 transition in ^{96}Sr. Moreover, the setup allowed for the re-measurement of the half-life of the 0_2^+ state in ^{96}Zr.

The γ-spectrum gated on the line at 219.1(3) keV – which corresponds to the E0 transition in ^{96}Sr – highlights both γ transitions at 414.3(1) keV and 814.9(2) keV, see Figure 14, which links the third excited 0^+ state to the

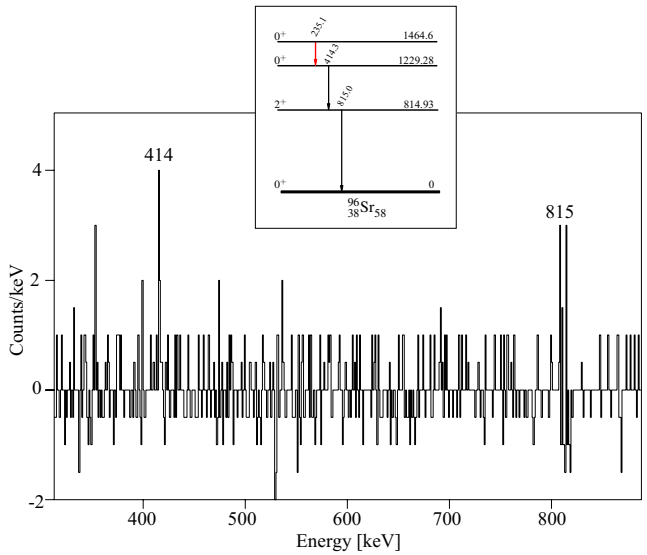

Figure 14: γ-spectrum gated on the E0 transition at 235.1 keV E0 in ^{96}Sr. The inset shows the partial level scheme of ^{96}Sr. Energies are in keV.

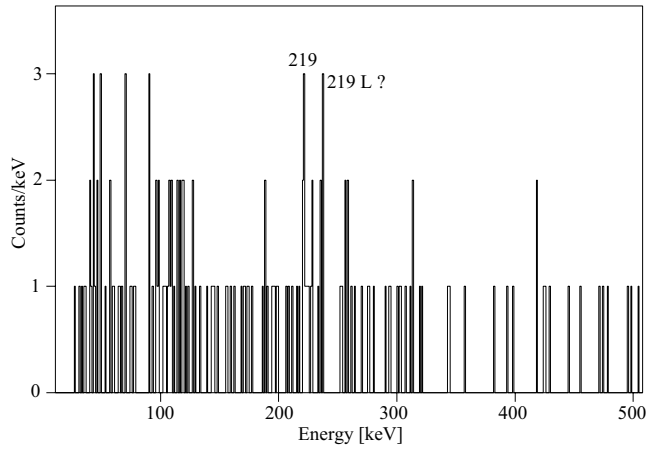

Figure 15: CE-spectrum gated on the γ transition at 414.3 keV transition in ^{96}Sr. The E0 transition at 235.1 keV is visible, while an accumulation of counts is also present at 233 keV, which could come from the conversion of electrons in the L-shell. Energies are in keV.

ground state, as shown on the partial level scheme in the inset. The inverse gate on the 414.3(1) keV line in the γ spectrum confirms the placement of the E0 transition, as a well defined peak is found at 219 keV, see Figure 15. A few counts are also seen at 233 keV that could belong to conversion electrons from the L shell, although due to a lack of statistics, this line is not observed in the gated electron spectrum.

One of the key elements to study nuclear structure with CE spectroscopy is the determination of the strength of the transition ρ_0. This quantity can be extracted from the half-life of the decaying states. Half-lives are extracted from the distribution of time difference between β events detected in the plastic scintillator and CE events in the

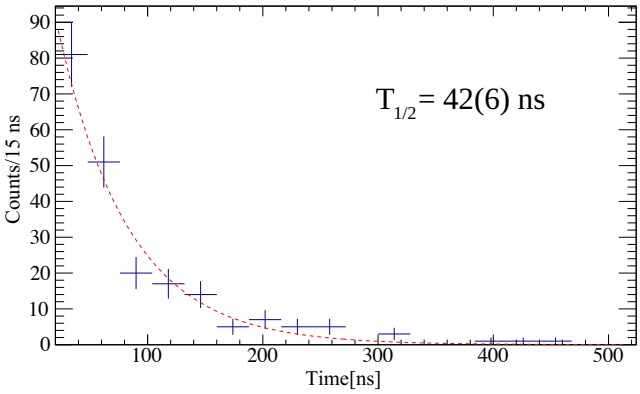

Figure 16: Projection on $\Delta T_{\beta-CE}$ of the E0 line at 1563.2 keV in the conversion electron spectrum of ^{96}Zr. The exponential fitting curve is drawn in red.

Si(Li) detector. The plastic scintillator and the Si(Li) detectors have a timing resolution of 1 ns and 15 ns respectively. The distribution of β-CE time difference is thus constructed with a 15 ns binning and allows the determination of half-lives of CE-decaying states in the tenth of nanoseconds range, with less than 15 % uncertainty, even with low statistics. Such a distribution is given for the CE line at 219 keV, fitted with a decreasing exponential, Figure 16, giving a half-life of $T_{1/2} = 42 \pm 6$ ns for the second 0^+ state in ^{96}Zr, in agreement with the adopted value of 38.0 ± 0.7 ns, taken as a weighted average of 38.0 ± 1.5 ns [16], 37.8 ± 1.2 ns [17] and 38.2 ± 1.2 ns [18].

5. Conclusion

A new setup for β-delayed conversion electron spectroscopy has been designed and built at IJCLab Orsay. It has been installed at the end of a dedicated radioactive beam line after the PARRNe mass-separator at ALTO. Its functioning is based on the collection of the beam on a movable tape and a magnetic transporter composed of two coils close to the Helmholtz configuration. The simulations used as a proof of concept and to dimension the setup as a whole were conducted using the COMSOL Multiphysics® software and are in agreement with measurements within 1 %. The absolute efficiency of the conversion electrons detection was determined using two standard sources of ^{207}Bi and ^{152}Eu placed as close to the collection point of the beam as possible. An online commissioning was conducted with a radioactive beam of ^{96}Rb and shows the possibilities offered by COeCO.

6. CRediT authorship contribution statement

G. Tocabens : Conceptualization, Formal analysis, Investigation, Writing – Original Draft, Validation. **C. Delafosse** : Supervision, Investigation, Writing - Review & Editing. **D. Verney** : Conceptualization, Supervision, Investigation, Writing - Review & Editing, Project administration. **E. Cantacuzène** : Investigation. **M. Cheikh**

Mhamed : Investigation. **I. Deloncle** : Investigation. **F. Didierjean** : Investigation. **W. Dong** : Investigation. **C. Gaulard** : Investigation, Resources. **B. Genolini** : Detector Design. **J. Guillot** : Investigation. **F. Hammache** : Investigation. **S. Harrouz** : Investigation. **F. Ibrahim** : Investigation. **H. Jacob** : Investigation. **M. Kaci** : Investigation. **A. de Lara** : Investigation. **N. de Séréville** : Investigation. **F. Le Blanc** : Investigation. **M. Lebois** : Investigation. **R. Lozeva** : Investigation. **I. Matea** : Investigation. **B. Roussière** : Investigation. **A. Segovia-Miranda** : Investigation. **R. Thoër** : Investigation.

7. Acknowledgments

The authors are most grateful to the ALTO teams for their strong commitment into the COeCO project, its construction and adaptation to the existing beamline. We express our special thanks to H. Ramarijaona from the Mechanical Engineering Department of IJCLab for all the work put in designing and the technical drawing of all the pieces. We would also like to thank B. Mathon, M. Imre and B. Geoffroy from the Mechanical Engineering Department of IJCLab for skillful manufacturing, assembling and mounting of the plastic scintillator as well as engineering plenty of mechanical pieces. Use of Ge detectors from the French-UK IN2P3-STFC Gamma Loan Pool and from the EXOGAM Collaboration is acknowledged.

References

[1] K. Heyde and R. A. Meyer. Monopole strength as a measure of nuclear shape mixing. *Phys. Rev. C*, 37:2170–2175, May 1988. doi: 10.1103/PhysRevC.37.2170.

[2] J. T. H. Dowie, T. Kibédi, T. K. Eriksen, and A. E. Stuchbery. Table of electronic factors for E0 electron and electron-positron pair conversion transitions. *Atom. Data Nucl. Data Tabl.*, 131: 101283, 2020. doi: 10.1016/j.adt.2019.06.002.

[3] Papadakis, P., Cox, D. M., O´Neill, G. G., Borge, M. J. G., Butler, P. A., Gaffney, L. P., Greenlees, P. T., Herzberg, R. -D., Illana, A., Joss, D. T., Konki, J., Kröll, T., Ojala, J., Page, R. D., Rahkila, P., Ranttila, K., Thornhill, J., Tuunanen, J., Van Duppen, P., Warr, N., and Pakarinen, J. The SPEDE spectrometer. *Eur. Phys. J. A*, 54(3):42, 2018. doi: 10.1140/epja/i2018-12474-9.

[4] E Zganjar. Conversion electron spectroscopy and its role in identifying shape coexisting structures in nuclei via E0 transitions. *Journal of Physics G: Nuclear and Particle Physics*, 43: 024013, 02 2016. doi: 10.1088/0954-3899/43/2/024013.

[5] J.M. Parmonen, Z. Janas, W.H. Trzaska, J. Äystö, J. Kantele, P.P. Jauho, A. Jokinen, and H. Penttilä. Electron-transporter spectrometer for on-line isotope separator. *Nuclear Instruments and Methods in Physics Research Section A: Accelerators, Spectrometers, Detectors and Associated Equipment*, 306(3):504 – 511, 1991. doi: 10.1016/0168-9002(91)90044-Q.

[6] N. Marchini, A. Nannini, M. Ottanelli, A. Saltarelli, M. Rocchini, G. Benzoni, E.R. Gamba, A. Goasduff, A. Gottardo, T. Krings, and M. Perri. SLICES: Spes Low-energy Internal Conversion Electron Spectrometer. *Nuclear Instruments and Methods in Physics Research Section A: Accelerators, Spectrometers, Detectors and Associated Equipment*, 1020:165860, 2021. ISSN 0168-9002. doi: https://doi.org/10.1016/j.nima.2021.165860.

[7] F. Ibrahim, D. Verney, M. Lebois, B. Roussière, S. Essabaa, S. Franchoo, S. Gales, D. Guillemaud Mueller, C. Lau, F. Le Blanc, J.F. Le Du, M.C. Mhamed, A.C. Mueller, and J. Sauvage. The ALTO facility at IPN Orsay and study of neutron rich nuclei in the vincinity of ^{78}Ni. *Nuclear Physics A*, 787 (1-4):110–117, 2007. doi: 10.1016/j.nuclphysa.2006.12.021.

[8] A. Gottardo, D. Verney, C. Delafosse, F. Ibrahim, B. Roussière, C. Sotty, S. Roccia, C. Andreoiu, C. Costache, M.-C. Delattre, I. Deloncle, A. Etilé, S. Franchoo, C. Gaulard, J. Guillot, M. Lebois, M. MacCormick, N. Marginean, R. Marginean, I. Matea, C. Mihai, I. Mitu, L. Olivier, C. Portail, L. Qi, L. Stan, D. Testov, J. Wilson, and D. T. Yordanov. First evidence of shape coexistence in the ^{78}Ni region: Intruder 0_2^+ state in ^{80}Ge. *Phys. Rev. Lett.*, 116:182501, May 2016. doi: 10.1103/PhysRevLett.116.182501.

[9] Saint-Gobain. BC-400,BC-404,BC-408,BC-412,BC-416 Premium Plastic Scintillators data-sheet, 2005.

[10] L. Thornill. Technologie des compteurs à scintillations. *CERN, Rapport Interne*, 83(5):1–38, 1983.

[11] Hamamatsu Photonics K.K. Metal package photomultiplier tube R7400U Series, 2001.

[12] COMSOL Multiphysics. URL. https://www.comsol.com/.

[13] G. Tocabens. *Conception et exploitation d'un dispositif pour la spectroscopie d'électrons de conversion β-retardés, application à l'étude de la région des noyaux riches en neutrons de masse A ∼ 100.* PhD thesis, université Paris-Saclay, 2022.

[14] Evaluated Nuclear Structure Data File. URL `https://www.nndc.bnl.gov/ensdf/`.

[15] Paul E. Garrett, Magda Zielińska, and Emmanuel Clément. An experimental view on shape coexistence in nuclei. *Progress in Particle and Nuclear Physics*, 124: 103931, 2022. doi: 10.1016/j.ppnp.2021.103931. URL `https://hal.science/hal-03584676`.

[16] D. Burch, P. Russo, H. Swanson, and E.G. Adelberger. Lifetime of the first excited state in ^{96}Zr. *Physics Letters B*, 40(3):357–359, 1972. ISSN 0370-2693. doi: https://doi.org/10.1016/0370-2693(72)90819-2.

[17] H. R. Andrews, J. S. Geiger, R. L. Graham, S. H. Sie, and D. Ward. Measurement of E0 transition probabilities for $0_1^+ \rightarrow 0^+$(g.s.) transitions in ^{94}Zr, ^{96}Zr and ^{100}Mo. *Bull.Am.Phys.Soc.*, 17:No.4, 514, EH11, 1972.

[18] H. R. Andrews, J. S. Geiger, R. L. Graham, S. H. Sie, and D. Ward. Electric monopole transition probabilities from 0^+ excited states. Technical Report AECL-4068,P54, uyg, 1971.

[19] G. Jung, B. Pfeiffer, P. Hungerford, S.M. Scott, F. Schussler, E. Monnand, J.A. Pinston, L.J. Alquist, H. Wollnik, and W.D. Hamilton. The level structure of ^{96}Y from the decay of ^{96}Sr. *Nuclear Physics A*, 352(1):1–12, 1981. ISSN 0375-9474. doi: https://doi.org/10.1016/0375-9474(81)90554-6.

[20] Saïd Essabaa, Nicole Barré-Boscher, Maher Cheikh Mhamed, Evelyne Cottereau, Serge Franchoo, Fadi Ibrahim, Christophe Lau, Brigitte Roussière, Abdelhakim Saïd, Sandrine Tusseau-Nenez, and David Verney. The radioactive beam facility ALTO. *Nuclear Instruments and Methods in Physics Research Section B: Beam Interactions with Materials and Atoms*, 317:218–222, 2013. doi: https://doi.org/10.1016/j.nimb.2013.06.029.

[21] J. A. BEARDEN and A. F. BURR. Reevaluation of X-Ray Atomic Energy Levels. *Rev. Mod. Phys.*, 39:125–142, Jan 1967. doi: 10.1103/RevModPhys.39.125.

Click here to access/download

LaTeX Source Files

Article_COeCO.zip

Declaration of interests

☒The authors declare that they have no known competing financial interests or personal relationships that could have appeared to influence the work reported in this paper.

☐The authors declare the following financial interests/personal relationships which may be considered as potential competing interests: